Proposal for observation of transitions induced by external magnetic fields mixing in the lower states: with an example from Fe X

Ran Si[1] , Wenxian Li[2], Tomas Brage[1,3,4] and Roger Hutton[3,4]

[1] Department of Physics, Lund University, Box 118, SE-22100 Lund, Sweden
[2] Department of Materials Science and Applied Mathematics, Malmö University, SE-20506, Malmö, Sweden
[3] Institute of Modern Physics, Fudan University, Shanghai 200433, People's Republic of China

E-mail: tomas.brage@fysik.lu.se and rhutton@fudan.edu.cn

CrossMark

Abstract

It is normally assumed that induced transitions, by e.g. hyperfine, magnetic field or spin interaction, arise due to mixing in the upper levels. In this paper we discuss an example when mixing in the lower levels through an externally applied magnetic field gives rise to a magnetic field induced transition. We discuss the theory for such a transition and give an example from Fe X, which is relevant for the determination of the magnetic field of the solar corona. To make this possible, it is important to determine the energy difference between the $3p^4 3d\ ^4D_{5/2}$ and $^4D_{7/2}$, which are accidentally very close in energy in Fe X. The splitting of these levels is expected to be around $3.5\,\mathrm{cm}^{-1}$ whereas their excitation energies are about $388\,709\,\mathrm{cm}^{-1}$. We discuss how this fine structure can be determined, by observing transitions from levels that decay into this pair which have a longer wavelength than the resonance transition. Finally we discuss an experimental scenario based on an electron beam ion trap and a Fabry–Perot interferometer, to perform the measurement of this interval.

(Some figures may appear in colour only in the online journal)

1. Introduction

Transitions induced by the presence of an external magnetic field (we will label these as MIT) were first observed by Beiersdorfer *et al* [1], through the $2p^5 3s\ ^3P_0 \rightarrow 2p^6\ ^1S_0$ transition in neon-like Argon, in an electron beam ion trap (EBIT). This initiated a new field of investigation and the MITs were recognized not only as a disturbance or source of error in measurements of long lifetimes [2–4] but also a new and rather exotic way of probing the structure of ions [5–13]. In all of these works the mixing that drives the transition is in the upper states, something that is a common assumption in

the search for 'unexpected transitions' [14, 15]. In this paper we will for the first time, to the best of our knowledge, analyze the possibility of observing an MIT induced by mixing in the lower states.

In three recent papers [10–12] we have discussed the use of spectral lines in the spectrum of Fe X as a diagnostic of the solar corona magnetic field strength. The line in question is induced by a close degeneracy between two upper levels within the $3p^4 3d\ ^4D$ term. In the absence of an external magnetic field, the $J = 7/2$ state of this term can only decay, radiatively, through an M2 forbidden transition, with a low rate of $A(7/2 \rightarrow 3/2) \approx 58\,\mathrm{s}^{-1}$. However the $^4D_{7/2}$ level is almost energy degenerate with the $^4D_{5/2}$ level, which has a spin-forbidden $E1$ transition, with a relatively large transition

[4] Authors to whom any correspondence should be addressed.

rate of $A(5/2 \rightarrow 3/2) \approx 6.0 \times 10^6\,\mathrm{s}^{-1}$, to the ground level, $3p^5\,{}^2P_{3/2}$. In the presence of an external magnetic field these two ${}^4D$ levels will mix and an $E1$ decay for the ${}^4D_{7/2}$ level will open as an MIT. The rate of this induced line is to first order given by

$$A_{\mathrm{MIT}} \propto \frac{B^2}{(\Delta E)^2}, \tag{1}$$

where B is the external magnetic field and ΔE is the energy splitting between the two ${}^4D$'s. It is clear that if we are aiming for a measurement of the external field in e.g. the solar corona, we need an accurate measurement of the 7/2–5/2 fine-structure energy, ΔE, a challenge since the transition to the ground state is in the VUV-region [10]. In [11] we extracted this fine structure energy by reversing the arguments presented in [10] for measuring the corona magnetic field, and used the known magnetic field of an EBIT, to extract a fine-structure energy of 3.5 cm^{-1} with the upper limit 7.8 cm^{-1}. In the most recent paper [12] we turned to transitions from above into the ${}^4D$'s, which are potentially in a longer wavelength region making it more plausible to resolve the fine structure ΔE. In that study we used unresolved transitions from the $3p^4 3d\,{}^2G_{7/2}$, which exhibits M1 transitions to both the ${}^4D_{5/2}$ and ${}^4D_{7/2}$ levels, independent of an external magnetic field. The resulting and refined fine-structure value was reported as $\Delta E = 3.6 \pm 2.7$ cm^{-1} using a recording from a spectrometer onboard the Skylab satellite [16].

In this work we have again refined the argument, and look for an MIT induced by a mixing in the lower levels. It is clear that these are harder to observe, in the general case, than when the mixing occur in the upper states, since the MIT has to have a similar A-value as the competing 'expected' line to be observable, i.e. to have a significant branching fraction from the upper level. Such an MIT could be expected if the upper level have e.g. $J = 9/2$. There are several candidates within the configuration $3p^4 3d$ but from consideration of observability of the transition and the resolvability of the ΔE, our choice is to investigate the decay of the $3p^4 3d\,{}^4F_{9/2}$ level in the presence of an external magnetic field. With no field the ${}^4F_{9/2}$ can only decay to the ${}^4D_{7/2}$ through an M1 transition, but not to the ${}^4D_{5/2}$ level (except through higher multipoles that have very low rates). But, as mentioned above, an external magnetic field will mix the ${}^4D_{5/2}$ level with the ${}^4D_{7/2}$ inducing an MIT from the ${}^4F_{9/2}$. The mixing coefficient between the ${}^4D_{5/2}$ and ${}^4D_{7/2}$ will be the same as in our previous work, however it will require a stronger magnetic field to induce the MIT as the rate of the $3p^4 3d\,{}^4F_{9/2} - 3p^4 3d\,{}^4D_{7/2}$ transition is much lower.

The transition between the ${}^4F_{9/2}$ and the ${}^4D_{7/2}$ has been observed and the lifetime has been measured to be 85.7 ± 9.2 ms [17] (to be compared to the lifetime of the $3p^4 3d\,{}^4D_{5/2}$ which is around 0.17 ns [18]). From this we can derive the rate to be $A(9/2 \rightarrow 7/2) \approx 11.7$ s^{-1}. This system is therefore an example where a magnetic field can be used to measure very small fine structure energies, especially when using an EBIT as the light source [11]. We have also identified a case when by using an MIT within the same configuration as the fine structure to be measured, the lines are in a longer wavelength region which relaxes the conditions on the spectrometer resolution.

Table 1. Number of CSFs in the final step of the core-valence model.

J	No. of CSFs
Even parity	
1/2	391377
3/2	761966
5/2	979034
7/2	972046
9/2	745228
Odd parity	
1/2	145486
3/2	325309

2. Theory I: The MCDHF approach

In the present work, the variational multiconfiguration Dirac–Hartree–Fock (MCDHF) method [19] implemented in the GRASP2K package [20] is adopted. The MCDHF method starts from a Dirac–Coulomb Hamiltonian H_{DC} and the electron correlation effect is included by expanding our Atomic State Function (ASF) in a linear combination of Configuration State Functions (CSFs). The one-electron orbitals and the expansion coefficients of the CSFs are obtained by the relativistic self-consistent field (RSCF) procedure. Each RCSF calculation is followed by a relativistic configuration interaction (RCI) calculation [21], where the Dirac orbitals are kept fixed, and only the expansion coefficients of the CSFs are determined by finding selected eigenvalues and eigenvectors of the complete interaction matrix. In this procedure, the transverse photon interaction and leading quantum electrodynamic (QED) effects (vacuum polarization and self-energy) are included.

To construct the CSF-space, configuration expansions are generated by single (S) and double (D) replacements of orbitals from the multi-reference set of configurations with ones in an active set of orbitals. The first multi-reference set consists of the configurations

$$3s^2 3p^5,\ 3s 3p^5 3d,\ 3s^2 3p^3 3d^2$$

for the odd states and

$$3s 3p^6,\ 3s^2 3p^4 3d,\ 3s 3p^4 3d^2,\ 3p^6 3d,\ 3s^2 3p^2 3d^3$$

for the even ones. These sets are used in a first step with an active set including orbitals with $n \leqslant 4$, $l \leqslant 3$. To extend the calculations further, only the first odd configuration and the first two even ones are used in the multi-reference set, while the active set is increased to include orbitals with $n \leqslant 7$, $l \leqslant 4$. By defining the $n = 3$ subshells as valence electrons,

Table 2. Magnetic field induced transition rates, A_{MIT} (in s^{-1}) and branching ratios (BR) for different magnetic field strengths, B (in T) and energy splittings, ΔE.

B	$\Delta E = 6$ cm^{-1}		$\Delta E = 3.5$ cm^{-1}		$\Delta E = 1$ cm^{-1}	
	A_{MIT}	BR	A_{MIT}	BR	A_{MIT}	BR
1	0.020	0.002	0.057	0.005	0.569	0.051
2	0.077	0.007	0.214	0.019	1.471	0.144
3	0.167	0.014	0.440	0.039	2.143	0.225
4	0.283	0.025	0.701	0.064	2.595	0.286
5	0.420	0.037	0.970	0.091	2.906	0.332
6	0.569	0.051	1.230	0.118	3.129	0.366
7	0.724	0.066	1.471	0.144	3.295	0.394
8	0.881	0.082	1.690	0.169	3.423	0.415

we treat the rest as a core. Based on this we included both valence-valence and core-valence correlation. In the latter calculations the 1*s* subshell is kept closed and therefore inactive, and only 2*s* and 2*p* are active core subshells. The total numbers of CSFs in our final core-valence calculation are listed in table 1.

3. Theory II: MIT-transitions

In a simple model of the rate of the unexpected [14, 15] transition that arises from the mixing of the two ^4D-levels, we will label these lower states in our calculations $|\frac{7}{2}M'\rangle$ and $|\frac{5}{2}M'\rangle$, where M' is the magnetic quantum number of the levels. From an upper state with $J = 9/2$, we can get an M1 transition to the former of these lower states (and a four orders of magnitude weaker E2 to the $J = 5/2$, which we will ignore). We will denote the rate of this expected, but forbidden transition as $A\left(\frac{9}{2}M \to \frac{7}{2}M'\right)$. However, in a magnetic field the two lower levels will interact leading to two mixed states

$$\left|\frac{`7'}{2}M'\right\rangle \approx c_1(M')\left|\frac{7}{2}M'\right\rangle + c_2(M')\left|\frac{5}{2}M'\right\rangle$$
$$\left|\frac{`5'}{2}M'\right\rangle \approx c_2(M')\left|\frac{7}{2}M'\right\rangle - c_1(M')\left|\frac{5}{2}M'\right\rangle, \quad (2)$$

where $c_1(M')$ and $c_2(M')$ are the mixing coefficients of the two levels, $|JM'\rangle$ and $|`J'M'\rangle$ stand for the levels before and after considering the mixing due to a magnetic field.

Since the upper state is not affected by the magnetic field, we can write the transition rates for the mixed states as

$$A\left(\frac{9}{2}M \to \frac{`7'}{2}M'\right) \approx |c_1(M')|^2 A\left(\frac{9}{2}M \to \frac{7}{2}M'\right)$$
$$A\left(\frac{9}{2}M \to \frac{`5'}{2}M'\right) \approx |c_2(M')|^2 A\left(\frac{9}{2}M \to \frac{7}{2}M'\right) \quad (3)$$

By using an updated version [22] of the HFSZEEMAN package [5] and diagonalizing the interaction matrix, we can get the Zeeman splitting of the fine-structure levels and mixing coefficients $c_1(M')$ and $c_2(M')$ in complete model, including all orders of the magnetic field perturbation. It is helpful, however, for the sake of argument, to consider the

Table 3. *M*-dependent wavelengths and rates for $J = 9/2$, $M \to J' = 7/2$, M' transitions at the magnetic field strengths of $B = 8$ T and energy splitting of $\Delta E = 3.5$ cm^{-1}.

$M \to M'$	$J = 9/2 \to J = 7/2$		$J = 9/2 \to J = 5/2$	
	λ (nm)	A (s^{-1})	λ (nm)	A (s^{-1})
$9/2 \to 7/2$	345.431	1.167		
$7/2 \to 7/2$	345.490	0.259		
$5/2 \to 7/2$	345.549	0.032		
$7/2 \to 5/2$	345.416	0.739	345.472	0.169
$5/2 \to 5/2$	345.475	0.369	345.531	0.084
$3/2 \to 5/2$	345.534	0.079	345.590	0.018
$5/2 \to 3/2$	345.407	0.530	345.475	0.150
$3/2 \to 3/2$	345.466	0.454	345.534	0.129
$1/2 \to 3/2$	345.525	0.151	345.593	0.043
$3/2 \to 1/2$	345.401	0.376	345.474	0.110
$1/2 \to 1/2$	345.460	0.502	345.533	0.146
$-1/2 \to 1/2$	345.518	0.251	345.592	0.073
$1/2 \to -1/2$	345.397	0.255	345.472	0.069
$-1/2 \to -1/2$	345.455	0.509	345.531	0.139
$-3/2 \to -1/2$	345.514	0.382	345.590	0.104
$-1/2 \to -3/2$	345.395	0.158	345.467	0.036
$-3/2 \to -3/2$	345.454	0.475	345.526	0.108
$-5/2 \to -3/2$	345.512	0.554	345.585	0.126
$-3/2 \to -5/2$	345.395	0.085	345.460	0.013
$-5/2 \to -5/2$	345.454	0.395	345.519	0.059
$-7/2 \to -5/2$	345.513	0.790	345.578	0.117
$-5/2 \to -7/2$	345.399	0.032		
$-7/2 \to -7/2$	345.458	0.259		
$-9/2 \to -7/2$	345.516	1.167		

simple first-order model, where $c_2(M')$ is given by

$$c_2(M') \approx -B\sqrt{\frac{49 - 4M'^2}{112}}\frac{\langle^4D_{5/2}||N^{(1)} + \Delta N^{(1)}||^4D_{7/2}\rangle}{E(^4D_{7/2}) - E(^4D_{5/2})}, \quad (4)$$

where the tensor operator $N^{(1)}$ represents the coupling of the electrons with the field, and $\Delta N^{(1)}$ is the Schwinger QED correction.

It is clear that the coefficients are dependent on the M' quantum number, but to be able to judge the importance of the MIT, we can define an approximate and average value of the mixing coefficient as

$$C_1^2 = \frac{\sum_M |c_1(M')|^2}{2J + 1}, \quad C_2^2 = \frac{\sum_M |c_2(M')|^2}{2J + 1}. \quad (5)$$

According to this we can list the branching ratio

$$\text{BR} = \frac{A(9/2 \to `5/2\text{'})}{A(9/2 \to `7/2\text{'})} = C_2^2/C_1^2 \quad (6)$$

of the two transitions for arbitrary field strengths B and energy splittings ΔE. We give some examples in table 2.

Under large magnetic fields, the Zeeman splitting and intensity redistributions can not be ignored. We show the wavelengths and rates of $J, M \to J', M'$ transitions in the case of $\Delta E = 3.5$ cm^{-1} and $B = 8$ T in table 3. The line profiles for different fine structure energy splittings in a magnetic field of 8 T are shown in figure 1, using a complete model.
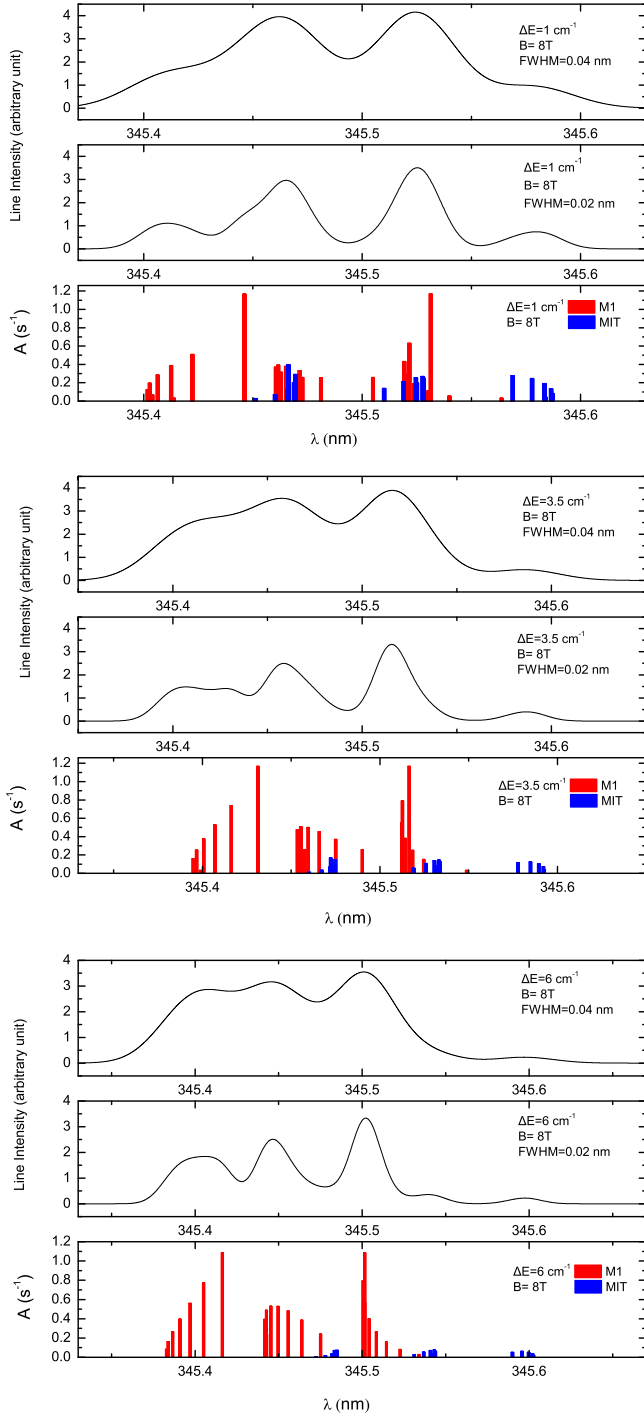
Figure 1. J, $M \to J'$, M' transition rates at $B = 8$ T and different energy splittings. The lower panels show the individual theoretical lines, the middle panels are convolved with Gaussian functions using a FWHM of 0.02 nm, while the upper panels are convolved using a FWHM of 0.04 nm.

4. Discussion

Visible spectra of iron in charge states close to Fe X were recently studied using an EBIT [23]. In figure 1 in [23] the Corona red line was clearly seen and its wavelength was measured with higher precision, compared to the NIST tabulated data, at 637.4538 nm. The line of interest in this

paper, the 345.42 nm line, has been seen in the Corona and is quite strong with an intensity of about 15% of the Corona red line [24]. However, it was not seen in the work done in [23] due to the fact that the electron beam energies were changed to optimize for Fe XI in the longer wavelength region.

The experiment we propose here would be to optimize the electron energy for Fe X and record spectra around the 345.42 nm line. Once the EBIT has been optimized for this line it can be isolated using a fairly commonly available spectrometer, e.g. the one used in [23]. It is important in this experiment to also optimize the spectral line widths as the most current and accurate measurement of the fine structure is only 3.6 ± 2.7 cm^{-1} [11]. This can be achieved by reducing the longitudinal trap depth, allowing the hotter ions to escape and hence minimizing the Doppler broadening. This leads to a compromise situation between Doppler broadening and line intensity. The final resolution should be provided by a Fabry–Perot interferometer. The spectrum shown in figure 1 of [23] shows that the corona red line (Fe X) is strong after 30 minutes of data collection (since in the solar corona it has an intensity of about 15% of the intensity of the red coronal line). The intensity of this line in an EBIT would depend strongly on the efficiency of the observing optics, but it is not likely that its intensity is restrictive to observation of the spectral feature. The important thing is that the signal rate is higher than the CCD dark rate, which for a cooled CCD is very low. It should be remembered that EBITs, albeit being weak light sources, can be run stably for long periods of time —up to days if needed.

In [10] we discussed Zeeman splitting in the MIT at the field strengths possible in the active solar corona and concluded that the influence was very small. However in the proposed laboratory experiment, we need to deploy a rather strong magnetic field of several Tesla, to reach an observable branching fraction for the MIT. Therefore the Zeeman splitting cannot be overlooked in the proposed experiment - as a matter of fact it will dominate the pattern seen by the Fabry–Perot interferometer.

In figure 1, we assume that the $^4D_{7/2}$ level is below, in energy, the $^4D_{5/2}$ level, as was assumed in the fine structure extraction from Solar data in [12]. For each value of the fine structure the top panel shows the result of convolving the data in the bottom panel, representing the theoretical results described in the earlier section, with a full width at half maximum (FWHM) of both 0.02 and 0.04 nm. The final value for the fine structure could be extracted by fitting the experimental data with a theoretical synthetic spectrum, where the fine structure is the only unknown parameter, according to standard procedures, and give an improved value for the fine structure.

5. Conclusion

We have presented the idea that unexpected transitions, i.e. transitions that arise due to mixing in wave functions, can occur when the lower levels mix, as opposed to the more commonly thought of mixing in the upper levels. We have

demonstrated this idea for levels in Fe X and for level mixing caused by an external magnetic field, the unexpected line then being what we call a magnetic induced transition. We have also discussed how this may be used to measure a very small fine structure energy difference for two levels in Fe X, the $^4D_{5/2}$ and $^4D_{7/2}$. An accurate value for this fine structure energy is necessary to enable a measurement of the magnetic field of the solar corona using another magnetic induced transitions in Fe X, originated from the $^4D_{7/2}$ levels, as discussed in our earlier work.

Acknowledgments

ORCID iDs

Ran Si ⬤ https://orcid.org/0000-0002-6206-4873
Tomas Brage ⬤ https://orcid.org/0000-0003-3985-767X

References

[1] Beiersdorfer P, Scofield J H and Osterheld A L 2003 *Phys. Rev. Lett.* **90** 235003
[2] Schef P, Lundin P, Biémont E, Källberg A, Norlin L O, Palmeri P, Royen P, Simonsson A and Mannervik S 2005 *Phys. Rev.* A **72** 020501
[3] Taichenachev A V, Yudin V I, Oates C W, Hoyt C W, Barber Z W and Hollberg L 2006 *Phys. Rev. Lett.* **96** 083001
[4] Crick D R, Donnellan S, Segal D M and Thompson R C 2010 *Phys. Rev. A* **81** 052503
[5] Andersson M and Jönsson P 2008 *Comput. Phys. Commun.* **178** 156
[6] Beiersdorfer P, Obst M and Safronova U I 2011 *Phys. Rev. A* **83** 012514
[7] Li J, Dong C, Jönsson P and Gaigalas G 2011 *Phys. Lett.* A **375** 914
[8] Li J, Grumer J, Li W, Andersson M, Brage T, Hutton R, Jönsson P, Yang Y and Zou Y 2013 *Phys. Rev. A* **88** 013416
[9] Grumer J, Li W, Bernhardt D, Li J, Schippers S, Brage T, Jönsson P, Hutton R and Zou Y 2013 *Phys. Rev. A* **88** 022513
[10] Li W, Grumer J, Yang Y, Brage T, Yao K, Chen C, Watanabe T, Jönsson P, Lundstedt H, Hutton R and Zou Y 2015 *Astrophys. J.* **807** 69
[11] Li W, Yang Y, Tu B, Xiao J, Grumer J, Brage T, Watanabe T, Hutton R and Zou Y 2016 *Astrophys. J.* **826** 219
[12] Judge P G, Hutton R, Li W and Brage T 2016 *Astrophys. J.* **833** 185
[13] Beiersdorfer P, López-Urrutia J R C and Trbert E 2016 *Astrophys. J.* **817** 67
[14] Brage T, Andersson M and Hutton R 2009 *AIP Conf. Proc.* **1125** 18
[15] Grumer J, Brage T, Andersson M, Li J, Jönsson P, Li W, Yang Y, Hutton R and Zou Y 2014 *Phys. Scr.* **89** 114002
[16] Bartoe J D F, Brueckner G E, Purcell J D and Tousey R 1977 *Appl. Opt.* **16** 879–86
[17] Moehs D P, Church D A, Bhatti M I and Perger W F 2000 *Phys. Rev. Lett.* **85** 38
[18] Wang K, Jönsson P, Zanna G D, Godefroid M, Chen Z B, Chen C Y and Yan J 2019 *Astrophys. J. Supple. Ser.* **246** 1
[19] Fischer C F, Godefroid M, Brage T, Jönsson P and Gaigalas G 2016 *J. Phys. B: At. Mol. Opt. Phys.* **49** 182004
[20] Jönsson P, Gaigalas G, Bieroń J, Fischer C F and Grant I 2013 *Comput. Phys. Commun.* **184** 2197
[21] McKenzie B, Grant I and Norrington P 1980 *Comput. Phys. Commun.* **21** 233
[22] Li W, Grumer J, Brage T and Jönsson P 2020 *Comput. Phys. Commun.* 107211 (in press)
[23] Bekker H, Hensel C, Daniel A, Windberger A, Pfeifer T and Crespo López-Urrutia J R 2018 *Phys. Rev. A* **98** 062514
[24] Jefferies J T, Orrall F Q and Zirker J B 1971 *Sol. Phys.* **16** 103